Appl Phys A (2009) 96: 283–287
DOI 10.1007/s00339-009-5202-6

Applied Physics A
Materials Science & Processing

Measurement of the optical Stark effect in semiconducting carbon nanotubes

Daohua Song · Feng Wang · Gordana Dukovic · Ming Zheng · E.D. Semke · Louis E. Brus · Tony F. Heinz

Received: 23 February 2009 / Accepted: 3 March 2009 / Published online: 28 March 2009

Abstract A strong optical Stark effect has been observed in (6,5) semiconducting single-walled carbon nanotubes by femtosecond pump-probe spectroscopy. The response is characterized by an instantaneous blueshift of the excitonic resonance upon application of pump radiation at photon energy well below the band gap. The large Stark effect is attributed to the enhanced Coulomb interactions present in these one-dimensional materials.

PACS 42.50.Hz · 71.35.-y · 78.67.Ch

1 Introduction

Intense optical radiation can alter the electronic structure of materials. One manifestation of such change is the shift of the optical transition energies of the system known as the optical Stark effect (OSE) [1]. This light–matter interaction was first observed in atoms [2, 3] and subsequently in molecular systems [4]. For many years, there has also been active research into the optical Stark effect in semiconductors [5–15]. Of particular interest are systems of reduced dimensionality where the radiation–exciton coupling is fundamentally altered by quantum-confinement effects and many-body interactions. This is exemplified in the detailed studies of two-dimensional quantum-well structures that have been reported in the literature [12, 13, 15]. It is consequently natural to extend these investigations to highly 1-dimensional (1-D) structures, where still stronger confinement and many-body effects are expected [16]. With diameters in the nanometer range, single-walled carbon nanotubes (SWNTs) [17, 18] provide an attractive model system for such studies. In addition, the optically excited states of SWNTs are characterized by strong excitonic interactions [19–21], which should enhance the optical transition moments and in turn lead to a large OSE.

In this paper, we report the identification and characterization of the optical Stark effect in single-walled carbon nanotubes of a defined chiral index (initial experimental results appear in [22]). The optical Stark effect was examined by means of femtosecond optical pump-probe spectroscopy. Our study complements earlier investigations of the transient optical response of SWNTs in which resonant or above band-gap pump excitation was employed to probe the ultrafast electron dynamics (for a recent overview, see [23]). Since the presence of real excitations easily masks the OSE, we isolate the response of the OSE by using pump excitation with photon energy far below the band gap. From the transient response probed by a white-light supercontinuum, we obtain a direct signature of the spectral shifts arising from the OSE. Other researchers have recently independently reported the presence of the optical Stark effect in the transient response of small diameter nanotubes under pump radiation slightly below the band gap [24, 25]. In addition to the use of pump radiation well below the band gap, our measurements

D. Song · F. Wang · T.F. Heinz (✉)
Departments of Physics and Electrical Engineering, Columbia University, New York, NY 10027, USA
e-mail: tony.heinz@columbia.edu

G. Dukovic · L.E. Brus
Department of Chemistry, Columbia University, New York, NY 10027, USA

M. Zheng · E.D. Semke
DuPont Central Research and Development, Wilmington, DE 19880, USA

Present address:
F. Wang · G. Dukovic
University of California at Berkeley, Berkeley, CA 94720, USA

are carried out in a purified sample consisting predominantly of nanotubes of just the (6,5) chiral index. This significantly simplifies the analysis and interpretation of the light-induced spectral changes. We observe an instantaneous blueshift of the E_{11} excitonic transition from which we obtain an accurate evaluation of the strength of the optical Stark effect. Adjusted for pump detuning within a two-level model, the observed OSE in SWNTs is one of the largest reported to date. We attribute its strength to the enhanced Coulomb interactions in the 1-D SWNTs.

2 Experimental

Our measurements were performed on a sample of purified SWNTs. The nanotubes were grown by chemical vapor deposition using the CoMoCAT process [26] and were subsequently processed by DNA-assisted dispersion and separation [27]. This treatment yields a sample consisting predominantly of (6,5) semiconducting nanotubes (diameter $d = 0.757$ nm, chiral angle $\theta = 27.0°$) with an average length of a fraction of micron. The isolated SWNTs were suspended in liquid D_2O in a 5-mm-thick cell. Deuterated water was chosen to provide optical transparency in the near-infrared to permit excitation at photon energies well below the nanotube transition energies. Figure 1 shows the optical absorption spectrum $\alpha_0(\hbar\omega)$ of the nanotube sample as a function of the photon energy $\hbar\omega$ around 1.2 eV. The principal feature at $\hbar\omega_0 = 1.253$ eV corresponds to the exciton associated with the lowest (E_{11}) sub-band transition of the (6,5) nanotube. The two weaker features at 1.280 and 1.336 eV arise from minor concentrations of other nanotube structures and have been assigned, respectively, to (8,3) and (9,1) chiral indices [28]. The presence of a single dominant resonance in the (6,5)-enriched sample, in contrast to the more complex spectra of the usual ensemble samples, greatly simplifies interpretation of the experimental Stark-shift data.

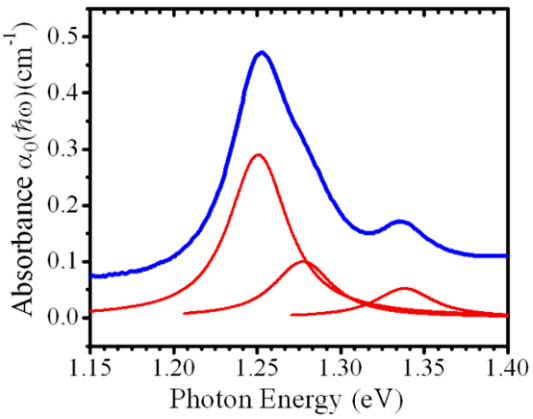

Fig. 1 Absorption spectrum $\alpha_0(\hbar\omega)$ of (6,5)-enriched solution of SWNTs as a function of photon energy (*blue curve*). The peak centered at 1.253 eV arises from the E_{11} excitonic transitions of (6,5) nanotubes. The *red curves* show the decomposition of this absorption into Lorentzian contributions from this nanotube species and weaker features from two minority nanotube species with absorption peaks at 1.280 and 1.336 eV

In our measurements, we employed a strong nonresonant pump beam at a photon energy of 0.69 eV and a weak continuum probe beam covering the E_{11} optical transition of the (6,5) nanotube. The laser apparatus for these pump-probe measurements was based on an amplified modelocked Ti:sapphire laser that delivered optical pulses of 130 fs duration at 800 nm. Part of this radiation was converted in an optical parametric amplifier to provide pump radiation at photon energy of $\hbar\omega = 0.69$ eV. This photon energy was chosen to be well below the nanotube E_{11} transition energy, as well as slightly below the threshold for two-photon absorption [19]. We probed the E_{11} transition of the nanotubes using a supercontinuum white-light radiation generated in a 2-mm-thick sapphire plate from a portion of the amplified Ti:sapphire beam. The probe beam was focused in the sample to a diameter of 0.2 mm, far smaller than the 2-mm pump spot. This permitted examination of the optical Stark effect under conditions of homogeneous excitation. Our probe spectra were recorded using a spectrometer equipped with a multichannel InGaAs detector. By comparing the absorption spectra with and without the pump radiation, we obtained the pump-induced change of the optical response of our sample. The dynamics of the light–matter interaction could also be studied by varying the time delay of the probe with respect to the pump pulse.

3 Results

3.1 Spectra

Figure 2 shows the change in the absorption spectrum of the nanotube sample induced by the optical pump radiation. The results (black curve) are presented as the differential sample absorbance measured with and without the pump radiation, $\Delta\alpha(\hbar\omega) \equiv \alpha_p(\hbar\omega) - \alpha_0(\hbar\omega)$. The measurements are obtained for temporally overlapping excitation and probe pulses, i.e., at zero time delay. In Fig. 2, we have also plotted the derivative of nanotube absorbance spectrum, $d\alpha_0/d(\hbar\omega)$, with respect to the photon energy (blue curve). For a rigid spectral shift of the features in the absorption spectrum that is small compared to the feature width, we expect $\Delta\alpha(\hbar\omega)$ to be proportional to $d\alpha_0/d(\hbar\omega)$. Such agreement is indeed observed.

The differential absorption spectrum is dominated by the 1.25 eV feature, the E_{11} response of the (6,5) nanotubes. There are also two weaker features around 1.28 and 1.34 eV. They arise from the optical Stark effects of the minority (8,3) and (9,1) nanotube structures, consistent with the absorption data. The agreement between the differential absorption and

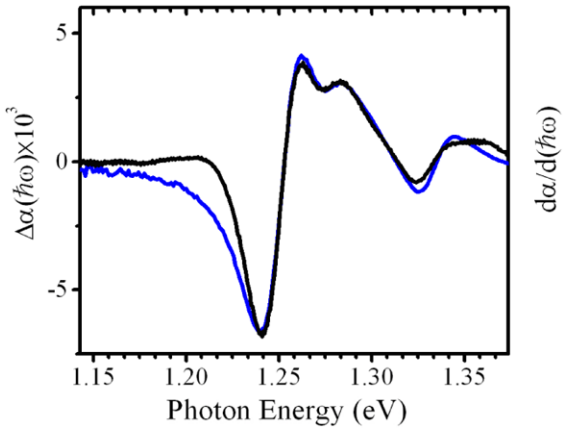

Fig. 2 Optically induced change in absorbance $\Delta\alpha(\hbar\omega) \equiv \alpha_p(\hbar\omega) - \alpha_0(\hbar\omega)$ of the nanotube sample for a pump intensity of 0.34 GW/cm^2 (*black trace*, left vertical axis). The probe is coincident with the pump in time. As expected for a small rigid shift of the absorption spectrum, $\Delta\alpha(\hbar\omega)$ matches the derivative of the absorption spectrum $d\alpha_0/d(\hbar\omega)$ (*blue trace*, right vertical axis) computed from data of Fig. 1

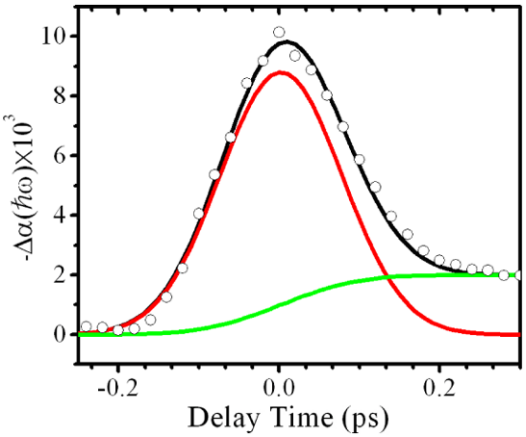

Fig. 3 Optically induced change in absorbance $\Delta\alpha(\hbar\omega) \equiv \alpha_p(\hbar\omega) - \alpha_0(\hbar\omega)$ of the nanotube sample probed at $\hbar\omega = 1.225$ eV as a function of pump-probe delay time. The experimental data are shown as *points*. The *black curve* is a fit to the data based on contributions from a dominant instantaneous optical Stark signal (*red curve*, with a width reflecting the experimental pump-probe cross-correlation signal) and a slow bleaching response from weak exciton generation by multiphoton absorption of the pump beam

the derivative of the absorption, including weaker features, indicates that their Stark shifts are comparable to that of the dominant (6,5) nanotube species. This result is not surprising given their similar transition energies and the significant detuning from resonance of the pump beam.

The minor discrepancy between the form of $\Delta\alpha(\hbar\omega)$ and $d\alpha_0/d(\hbar\omega)$ seen in Fig. 2 for lower photon energies is attributed to the presence of a weak background absorbance in the sample that does not display a significant Stark shift. Comparing the magnitude of experimental Stark spectrum $\Delta\alpha(\hbar\omega)$ and the calculated $d\alpha_0/d(\hbar\omega)$, we can determine, as discussed later in the paper, the magnitude and sign of the Stark shift. We separately confirmed the expected linearity of the Stark shift as a function of pump intensity for a range of 0.3–3 GW cm^{-2}.

3.2 Time-resolved measurements

In addition to the spectral signature of the optical Stark effect, we have further investigated the time-domain characteristics of the optical response. The transient absorption as a function of the probe delay time with respect to the pump pulse is presented in Fig. 3. The frequency shift of the features is found to be instantaneous within the resolution of the optical pump and probe pulses. This result confirms that the response is from the optical Stark effect. We also observe a weak transient bleaching at longer probe delay time. This response has a different spectral signature, corresponding to a reduction in strength rather than a shift of the optical transition energy. We attribute it to a band-filling effect from the weak excitation of real carriers through multiphoton absorption [19]. The analogous bleaching effect has also been observed in quantum-well systems [13]. Figure 3 shows the decomposition of the measured response as an instantaneous Stark shift and a weak transient bleaching, which is taken to have an infinite lifetime.

3.3 Magnitude of the optical Stark effect

To characterize the magnitude of the OSE in SWNTs, we need to consider the polarization effects. The 1-D character of the SWNTs leads to an highly anisotropic optical response: For a given SWNT light polarized along the nanotube produces much stronger excitation than light polarized perpendicular to the nanotube because of local-field screening effects [29]. Indeed, in practice, we can neglect interactions of light polarized perpendicular to the nanotube and can characterize the OSE by a single parameter describing the Stark shift in a nanotube aligned along the direction of the pump electric field, which we denote by $\delta(\hbar\omega_0)$. This quantity is related to the experimentally measured response of an isotropic sample of nanotubes in suspension through

$$\begin{aligned} \Delta\alpha_{\parallel} &= (3/5)\left[d\alpha_0/d(\hbar\omega)\right]\delta(\hbar\omega_0), \\ \Delta\alpha_{\perp} &= (1/5)\left[d\alpha_0/d(\hbar\omega)\right]\delta(\hbar\omega_0). \end{aligned} \tag{1}$$

Here $\Delta\alpha_{\parallel}(\hbar\omega)$ and $\Delta\alpha_{\perp}(\hbar\omega)$ are the experimentally measured differential absorbance for pump and probe radiation of parallel and perpendicular polarization, respectively, and $\alpha_0(\hbar\omega)$ is the absorbance of the unperturbed sample. The equation predicts a ratio of $\Delta\alpha_{\parallel}/\Delta\alpha_{\perp}$ of 3, which was confirmed by our experimental observations. With the experimentally determined values for $\Delta\alpha_{\parallel}$ and α_0, one can then deduce the optical Stark shift of a properly aligned nanotube, $\delta(\hbar\omega_0)$. After taking into account the spatial and temporal profiles of the pump and probe beams, we obtain a

spectral shift of $\delta(\hbar\omega_0) = 2.5$ meV for a pump intensity of 1 GW/cm^2.

4 Discussion

Since the optical properties are dominated by the 1-D excitonic transitions [19, 20], the OSE in carbon nanotubes can be described within an effective dressed-exciton picture. In the simplest approximation, we consider only a two-level system consisting of the vacuum as the ground state and the E_{11} exciton as the excited state. This treatment permits a convenient comparison with measurements of other material systems. Within this approximation, the optical Stark shift $\delta(\hbar\omega_0)$ is given by [3]

$$\delta(\hbar\omega_0) = \frac{\mu^2 E_\mathrm{p}^2}{\hbar\Omega}. \tag{2}$$

Here μ denotes the transition dipole moment between the two states of the system; E_p is the electric field of pump laser; and $\hbar\Omega = \hbar\omega_0 - \hbar\omega_\mathrm{p}$ represents the detuning between the energy of the exciton transition and that of the pump radiation. Even when the two-level system picture is not strictly valid, one expects the dependence of Stark shift on laser intensity I and Ω in (2) to hold roughly, provided that the two states play a dominant role.

Following (2) we can define an intrinsic measure of the material optical Stark effect strength as $S \equiv \delta(\hbar\omega_0)\hbar\Omega/2E_\mathrm{p}^2$, i.e., the magnitude of the optical Stark effect corrected for the pump intensity and laser detuning. We can compare its value in nanotube with other materials systems, such as semiconductor quantum wells and organic molecules. The results of such comparisons are listed in Table 1, together with the relevant parameters for previous measurements reported in the literature. Among these material systems, SWNTs exhibit the largest optical Stark effect as described by the S parameter.

Within the two-level model, the parameter S can be identified as the square of the transition dipole moment, μ^2. Using our experimental values, we then infer a transition dipole moment of $\mu = 12$ Debye for the (6,5) SWNT species at room temperature. This transition dipole moment is quite large. The strength of the optical transition can be understood as a result of enhanced Coulomb interactions in the 1-D nanotube structure. For Wannier excitons, the exciton transition strength scale with the probability of the overlap of the electron and hole, i.e., in 1-D, with the inverse of exciton Bohr radius, a_B^{-1} [30]. A strong electron–hole Coulomb interaction is thus advantageous for a large transition dipole moment because it leads to excitons with small Bohr radius a_B.

Within the same framework, our measured exciton transition dipole moment can be converted to an integrated exciton absorption cross section σ_exc through the standard relation for a localized radiating system [31], namely:

$$\sigma_\mathrm{exc} = \frac{3\pi\omega}{\varepsilon_0\hbar c}\mu^2. \tag{3}$$

For $\mu = 12$ Debye, we then deduce $\sigma_\mathrm{exc} = 7.5 \times 10^{-17}$ cm^2 eV. Because of the coherence of the exciton in nanotube (and extended solids generally), this value reflects the overall contribution of all of the carbon atoms included within the exciton coherence length l. As such, information about the exciton coherence length can be extracted by comparing σ_exc and the integrated absorption cross section per carbon atom σ_0, a quantity available through linear absorption measurements. The coherence length l links these two quantities through

$$\sigma_\mathrm{exc} = nl\sigma_0, \tag{4}$$

where n is the density of carbon atom per unit length. In the previous experiments [32], the absolute absorption cross section per carbon atom for E_{22} transition has been reported.

Table 1 Comparisons between the optical Stark effect in SWNTs measured in this work and values for several other material systems reported in the literature. The table shows the temperature of the sample, the detuning energy $\hbar\Omega$ of the pump photon below the resonance, the pump intensity, and the resulting optical Stark shift $\delta(\hbar\omega_0)$ and normalized Stark effect $S \equiv c\delta(\hbar\omega_0)\hbar\Omega/2I$, corrected for the laser intensity and detuning. For the case of the SWNTs, the values correspond to pump and probe pulses polarized along the nanotube axis. A similar adjustment for orientation has been applied to values for rhodamine B molecules

Material	Temperature (K)	Detuning $\hbar\Omega$ (meV)	Pump intensity I (GW cm^{-2})	Optical Stark shift $\delta(\hbar\omega_0)$ (meV)	S (Debye^2)
SWNT	300	560	1.0	2.5	140
GaAlAs quantum well [13]	70	40	0.010	0.1	41
InGaAs quantum well [14]	80	20	0.010	0.19	39
Rhodamine B [4]	300	200	25	25	21

By integrating over the excitonic transition and using experimental absorption data to determine the ratio of the E_{11} strength compared to that of the E_{22} transition, we estimate the integrated E_{11} absorption per carbon atom for (6,5) nanotube as $\sigma_0 = 4\text{–}8 \times 10^{-19}$ cm^2 eV per carbon atom. From this value, we infer a room-temperature exciton coherence length of $l = 2\text{–}4$ nm. We expect that this length would increase with decreasing temperature leading to an enhancement in σ_{exc} and, correspondingly, in the magnitude of OSE.

Although we have introduced a simple two-level model for discussion of our OSE results, further theoretical analysis will be required for a quantitative understanding of the response of SWNTs. In particular, the two-level model neglects the interactions between virtual excitons and the complete nanotube electronic structure. The continuum states near the E_{11} excitonic transition and higher-lying excitons associated with other sub-bands may significantly alter the OSE. In addition, the role of strong Coulomb effects, which has only been considered perturbationally in previous theoretical investigations of 2-D semiconductors [15, 33], may be of more central importance in a complete description of the OSE in carbon nanotubes. We hope that our experiment will stimulate further theoretical study of the distinctive optical response of such 1-D systems.

5 Conclusions

We have applied two-color femtosecond pump-probe spectroscopy to examine the optical Stark effect in a sample consisting of (6,5) semiconducting SWNTs. This prototype 1-D system exhibited an optical Stark shift for the E_{11} exciton of 2.5 meV/(GW cm^{-2}) when subjected to pump radiation at photon energies well below this transition. Corrected for pump detuning, this is among the largest optical Stark effects reported in any material. The large optical Stark effect is attributed to the strong Coulomb interaction between charge carriers in the nanotubes. We have presented a discussion of the optical Stark effect in carbon nanotubes in terms of a simple two-level model; a full multilevel analysis of the problem, taking into account the strong many-body interactions, remains an open theoretical problem.

Acknowledgements We thank Dr. Yi Rao for experimental assistance. We acknowledge the support from the Nanoscale Science and Engineering Initiative of the NSF (CHE-0117752), by the New York State Office of Science, Technology, and Academic Research (NYSTAR), and by the Office of Basic Energy Sciences, US Department of Energy (grants DOE-FG02-98ER14861 and DE-FG02-03ER15463).

References

1. Y.R. Shen, *The Principles of Nonlinear Optics* (Wiley, New York, 2002)
2. C. Cohen-Tannoudji, S. Reynaud, J. Phys. B **10**, 345–363 (1977)
3. C. Cohen-Tannoudji, Metrologia **13**, 161–166 (1977)
4. P.C. Becker, R.L. Fork, C.H.B. Cruz, J.P. Gordon, C.V. Shank, Phys. Rev. Lett. **60**, 2462–2464 (1988)
5. D. Frohlich, A. Nothe, K. Reimann, Phys. Rev. Lett. **55**, 1335–1337 (1985)
6. D. Hulin, A. Mysyrowicz, A. Antonetti, A. Migus, W.T. Masselink, H. Morkoc, H.M. Gibbs, N. Peyghambarian, Phys. Rev. B **33**, 4389–4391 (1986)
7. D. Frohlich, K. Reimann, R. Wille, J. Lumin. **38**, 235–238 (1987)
8. M. Combescot, R. Combescot, Phys. Rev. B **40**, 3788–3801 (1989)
9. O. Betbeder-Matibet, M. Combescot, Solid State Commun. **77**, 745–749 (1991)
10. F.Y. Qu, P.C. Morais, Phys. Lett. A **310**, 460–464 (2003)
11. C. Avendano, J.A. Reyes, M. del Castillo-Mussot, G.J. Vazquez, H. Spector, Chin. J. Phys. **42**, 751–763 (2004)
12. A. Mysyrowicz, D. Hulin, A. Antonetti, A. Migus, Phys. Rev. Lett. **56**, 2748–2751 (1986)
13. A. Von Lehmen, D.S. Chemla, J.E. Zucker, J.P. Heritage, Opt. Lett. **11**, 609–611 (1986)
14. K. Tai, J. Hegarty, W.T. Tsang, Appl. Phys. Lett. **51**, 152–154 (1987)
15. D.S. Chemla, W.H. Knox, D.A.B. Miller, S. Schmittrink, J.B. Stark, R. Zimmermann, J. Lumin. **44**, 233–246 (1989)
16. F. Rossi, E. Molinari, Phys. Rev. B **53**, 16462–16473 (1996)
17. R. Saito, M. Dresselhaus, M.S. Dresselhaus, *Physical Properties of Carbon Nanotubes* (Imperial College Press, London, 1998)
18. S. Reich, C. Thomsen, J. Maultzsch, *Carbon Nanotubes: Basic Concepts and Physical Properties* (Wiley, New York, 2004)
19. F. Wang, G. Dukovic, L.E. Brus, T.F. Heinz, Science **308**, 838–841 (2005)
20. J. Maultzsch, R. Pomraenke, S. Reich, E. Chang, D. Prezzi, A. Ruini, E. Molinari, M.S. Strano, C. Thomsen, C. Lienau, Phys. Rev. B **72**, 241402 (2005)
21. G. Dukovic, F. Wang, D.H. Song, M.Y. Sfeir, T.F. Heinz, L.E. Brus, Nano Lett. **5**, 2314–2318 (2005)
22. D.H. Song, F. Wang, G. Dukovic, M. Zheng, E.D. Semke, L.E. Brus, T.F. Heinz, in *Ultrafast Phenomena XV*, ed. by P. Corkum, D. Jonas, D. Miller, W.M. Weiner (Springer, Heidelberg, 2006), pp. 674–676
23. Y.Z. Ma, T. Hertel, Z.V. Vardeny, G.R. Fleming, L. Valkunas, in *Carbon Nanotubes*, ed. by A. Jorio, G. Dresselhaus, M.S. Dresselhaus (Springer, Heidelberg, 2008), pp. 321–352
24. S. Matsumoto, H. Matsui, A. Maeda, T. Takenobu, Y. Iwasa, Y. Miyata, H. Kataura, Y. Maniwa, H. Okamoto, Jpn. J. Appl. Phys. **45**, L513–L515 (2006)
25. A. Maeda, S. Matsumoto, H. Kishida, T. Takenobu, Y. Iwasa, H. Shimoda, O. Zhou, M. Shiraishi, H. Okamoto, J. Phys. Soc. Jpn. **75**, 043709 (2006)
26. S.M. Bachilo, L. Balzano, J.E. Herrera, F. Pompeo, D.E. Resasco, R.B. Weisman, J. Am. Chem. Soc. **125**, 11186–11187 (2003)
27. M. Zheng, A. Jagota, M.S. Strano, A.P. Santos, P. Barone, S.G. Chou, B.A. Diner, M.S. Dresselhaus, R.S. McLean, G.B. Onoa, G.G. Samsonidze, E.D. Semke, M. Usrey, D.J. Walls, Science **302**, 1545–1548 (2003)
28. M.S. Arnold, S.I. Stupp, M.C. Hersam, Nano Lett. **5**, 713–718 (2005)
29. M.Y. Sfeir, F. Wang, L.M. Huang, C.C. Chuang, J. Hone, S.P. O'Brien, T.F. Heinz, L.E. Brus, Science **306**, 1540–1543 (2004)
30. R.J. Elliott, Phys. Rev. **108**, 1384–1389 (1957)
31. R.C. Hilborn, Am. J. Phys. **50**, 982–986 (1982)
32. M.F. Islam, D.E. Milkie, C.L. Kane, A.G. Yodh, J.M. Kikkawa, Phys. Rev. Lett. **93**, 037404 (2004)
33. M. Combescot, Phys. Rep. **221**, 167–249 (1992)